

# Mechanism and Kinetics of Inducible Nitric Oxide Synthase Auto-S-nitrosation and Inactivation

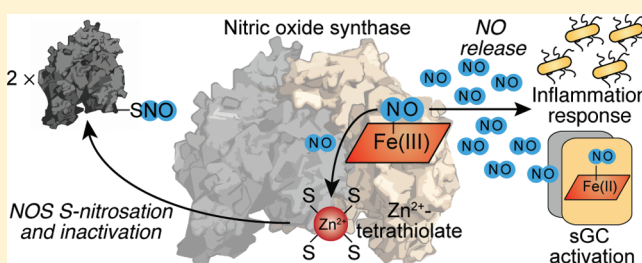
Brian C. Smith,<sup>†</sup> Nathaniel B. Fernhoff,<sup>‡</sup> and Michael A. Marletta<sup>\*,§,†,‡,||</sup>

<sup>†</sup>California Institute for Quantitative Biosciences, <sup>‡</sup>Department of Molecular and Cell Biology, <sup>§</sup>Department of Chemistry, and

<sup>||</sup>Division of Physical Biosciences, Lawrence Berkeley National Laboratory, University of California, Berkeley, California 94720-3220, United States

## S Supporting Information

**ABSTRACT:** Nitric oxide (NO), the product of the nitric oxide synthase (NOS) reaction, was previously shown to result in S-nitrosation of the NOS Zn<sup>2+</sup>-tetrathiolate and inactivation of the enzyme. To probe the potential physiological significance of NOS S-nitrosation, we determined the inactivation time scale of the inducible NOS isoform (iNOS) and found it directly correlates with an increase in the level of iNOS S-nitrosation. A kinetic model of NOS inactivation in which arginine is treated as a suicide substrate was developed. In this model, NO synthesized at the heme cofactor is partitioned between release into solution (NO release pathway) and NOS S-nitrosation followed by NOS inactivation (inactivation pathway). Experimentally determined progress curves of NO formation were fit to the model. The NO release pathway was perturbed through addition of the NO traps oxymyoglobin (MbO<sub>2</sub>) and  $\beta$ 2 H-NOX, which yielded partition ratios between NO release and inactivation of  $\sim 100$  at 4  $\mu$ M MbO<sub>2</sub> and  $\sim 22000$  at saturating trap concentrations. The results suggest that a portion of the NO synthesized at the heme cofactor reacts with the Zn<sup>2+</sup>-tetrathiolate without being released into solution. Perturbation of the inactivation pathway through addition of the reducing agent GSH or TCEP resulted in a concentration-dependent decrease in the level of iNOS S-nitrosation that directly correlated with protection from iNOS inactivation. iNOS inactivation was most responsive to physiological concentrations of GSH with an apparent  $K_m$  value of 13 mM. NOS turnover that leads to NOS S-nitrosation might be a mechanism for controlling NOS activity, and NOS S-nitrosation could play a role in the physiological generation of nitrosothiols.



Nitric oxide (NO) plays essential and disparate roles in mammalian physiology, causing vasodilation in the cardiovascular system, neurotransmission in nervous tissue, and cytotoxicity against pathogens in the immune response. NO is synthesized by nitric oxide synthase (NOS), which catalyzes the conversion of arginine to citrulline and NO, using oxygen (O<sub>2</sub>) and NADPH as cosubstrates.<sup>1</sup> Mammals possess three NOS isoforms: neuronal (nNOS), inducible (iNOS), and endothelial (eNOS). As a signaling agent, low nanomolar NO concentrations are synthesized by eNOS or nNOS. As a cytotoxin, micromolar NO concentrations are generated by iNOS at sites of infection or inflammation.<sup>2</sup>

All three NOS isoforms are dimeric and share a common architecture, composed of two domains: a reductase domain and an oxidase domain. The reductase domain contains flavin cofactors FAD and FMN and a binding site for cosubstrate NADPH, and shuttles electrons from NADPH to the oxidase domain of the opposite monomer in the dimer during catalysis. Therefore, NOS is active only as a homodimer. The oxidase domain binds the substrate arginine as well as the heme and tetrahydrobiopterin (H<sub>4</sub>B) cofactors. The interface of the oxidase domain homodimer contains a Zn<sup>2+</sup>-tetrathiolate that is comprised of two cysteines from each monomer.

In its classical signaling role, NO is captured by the heme cofactor of soluble guanylate cyclase (sGC), activating sGC to produce the secondary messenger cyclic GMP (cGMP).<sup>3</sup> However, mounting evidence points toward an alternative, cGMP-independent NO signaling pathway in which the S-nitrosation of cysteine residues regulates protein structure and activity.<sup>4</sup> S-Nitrosation has been implicated in a broad spectrum of diseases, including cancer, diabetes, and other cardiovascular, pulmonary, and neurological disorders,<sup>4</sup> yet the mechanism by which nitrosothiols are formed *in vivo* is unknown.

The direct transfer of a nitrosyl group from a nitrosothiol to a free thiol (i.e., transnitrosation) is a simple bimolecular reaction. However, the initial formation of a nitrosothiol from NO and a free thiol requires a one-electron oxidation. Transnitrosation reactions therefore necessitate an “initiating” nitrosothiol formed by a protein that uses NO and a free thiol to synthesize a nitrosothiol with the aid of an oxidant. The mitochondrial hemoprotein cytochrome *c* was recently shown to satisfy these criteria using NO, glutathione (GSH), and ferric

Received: December 9, 2011

Revised: January 6, 2012

Published: January 9, 2012



heme to form S-nitrosoglutathione (GSNO).<sup>5,6</sup> However, the high  $K_m$  value of NO and the high protein concentration utilized to observe this reaction suggest that another protein is responsible for the physiological generation of nitrosothiols at the lower NO concentrations commonly found in vivo. Cytochrome *c* may play a more significant role at the high NO levels encountered during nitrosative stress.

NOS is a potential candidate for the initial formation of nitrosothiols as all three mammalian NOS isoforms selectively form nitrosothiols at their Zn<sup>2+</sup>-tetrathiolate cysteines.<sup>7–11</sup> iNOS S-nitrosation dissociates the iNOS dimer, inactivates the enzyme, and may expose the nitrosothiols for transnitrosation reactions.<sup>8</sup> If involved in S-nitrosation, NOS must balance participation in this pathway against enzyme inactivation. Of the three NOS isoforms, only iNOS has been shown to participate in protein–protein interaction-mediated S-nitrosation reactions. Kim et al. showed that formation of an iNOS–cyclooxygenase-2 (COX-2) complex was required for S-nitrosation of COX-2.<sup>12</sup> Furthermore, procaspase-3 and iNOS participate in an NO-dependent protein–protein interaction.<sup>13</sup> As caspase-3 is known to be nitrosated on its active-site cysteine,<sup>14</sup> iNOS might directly transnitrosate caspase-3. Additionally, a protein–protein complex between iNOS and arginase-1 was shown to be necessary for arginase-1 S-nitrosation.<sup>15</sup>

Once formed, nitrosothiols can be transferred to downstream targets by formation of specific protein–protein or protein–small molecule interactions in a process analogous to phosphoryl transfer.<sup>16</sup> Mirroring the role of ATP in phosphorylation, transnitrosation reactions may involve a small molecule nitrosothiol donor. GSH is the most abundant thiol in mammalian cells (physiological concentrations range from 0.5 to 10 mM),<sup>17</sup> and GSNO has been detected both intra- and extracellularly.<sup>18–20</sup> Furthermore, GSNO can specifically transnitrosate thioredoxin,<sup>21,22</sup> and GSNO reductase knockout mice have markedly increased levels of S-nitrosated proteins.<sup>4</sup> As NOS is S-nitrosated and can participate in transnitrosation reactions, NOS may also be responsible, at least in part, for the physiological generation of GSNO.

Here, we performed a detailed kinetic analysis of iNOS S-nitrosation and inactivation by treating arginine as a suicide substrate. This model allowed direct determination of the partition ratio between the release of NO into solution and iNOS S-nitrosation followed by inactivation. Further insight was gained by perturbing this partition ratio through varying the concentration of arginine, NO traps, or reductants. Our results indicate that the main mechanism of iNOS inactivation is S-nitrosation of the Zn<sup>2+</sup>-tetrathiolate. We hypothesize that a tunnel, present in all three NOS isoforms, acts as a conduit between the heme and Zn<sup>2+</sup>-tetrathiolate and facilitates this S-nitrosation. Our kinetic results have implications for iNOS S-nitrosation as an initial source of nitrosothiols such as GSNO.

## EXPERIMENTAL PROCEDURES

**General Materials.** All chemicals used were of the highest purity commercially available and were purchased from Sigma (St. Louis, MO), Aldrich (Milwaukee, WI), or Fisher Scientific (Pittsburgh, PA) unless otherwise noted below.

**Protein Expression, Purification, and Preparation.** Expression and purification of murine iNOS (coexpressed with calmodulin)<sup>8,23</sup> and  $\beta$ 2 H-NOX<sup>24</sup> were conducted as described previously. iNOS concentrations were determined using the method of Bradford with bovine serum albumin as the

standard.<sup>25</sup> Horse heart myoglobin was purchased from Sigma. Horse heart oxymyoglobin (MbO<sub>2</sub>) was generated through dithionite reduction and desalting as described previously for oxymyoglobin.<sup>26</sup> Oxymyoglobin concentrations were determined using a heme extinction coefficient of 13.9 mM<sup>−1</sup> cm<sup>−1</sup> at 542 nm.<sup>27</sup> Generation of horse heart apomyoglobin by acidification to pH 2 with 0.1 N HCl and heme extraction with methyl ethyl ketone was performed as described previously.<sup>28</sup> Apomyoglobin concentrations were determined using an extinction coefficient of 15.5 mM<sup>−1</sup> cm<sup>−1</sup> at 280 nm.<sup>29</sup>

**iNOS Activity Assays.** Horse heart MbO<sub>2</sub> assays were conducted as previously described for NOS oxymyoglobin assays<sup>26</sup> with the following modifications. This assay monitors the absorbance change upon reaction of MbO<sub>2</sub> with NO to form nitrate and metmyoglobin (metMb). Assays were monitored at either 401, 540, or 581 nm in 300  $\mu$ L total volumes in clear 96-well microplates. Because of the strong absorbance of myoglobin at 401 nm, assays with MbO<sub>2</sub> concentrations of > 15  $\mu$ M were monitored at 540 or 581 nm. Activities were determined using an extinction coefficient of 45.5 mM<sup>−1</sup> cm<sup>−1</sup> for the increase in absorbance at 401 nm, 7.5 mM<sup>−1</sup> cm<sup>−1</sup> for the decrease in absorbance at 540 nm, or 10.5 mM<sup>−1</sup> cm<sup>−1</sup> for the increase in absorbance at 581 nm. These extinction coefficients were determined by the difference spectrum of horse heart MbO<sub>2</sub> and metMb (formed by reaction of MbO<sub>2</sub> with NO) at known initial MbO<sub>2</sub> concentrations.

**Biotin Switch Method.** The biotin switch method<sup>11</sup> was employed to assay S-nitrosation of iNOS. To avoid nitrosothiol decomposition, samples were protected from direct sunlight as much as possible. Assays contained 1–4  $\mu$ M iNOS, 5 mM Arg, 2 mM NADPH, and 50 mM NaCl with or without GSH/TCEP in either 50 mM HEPES or HEN buffer (250 mM HEPES, 2 mM EDTA, and 0.2 mM neocuproine) at pH 7.5 in total volumes of 100  $\mu$ L. iNOS S-nitrosation was initiated by addition of NADPH and quenched by addition of 100  $\mu$ L of blocking buffer (10% SDS and 60 mM N-ethylmaleimide in HEN buffer) and incubated at 55 °C for 30 min. The protein was then precipitated with 1.2 mL of acetone precooled to −20 °C and pelleted at 14000 rpm for 10 min at 4 °C. The supernatant was removed; the pellet was washed with an additional 0.9 mL of acetone, and the pellets were air-dried. Dried pellets were resuspended in PBS with 5% SDS, 30 mM ascorbate, and 500  $\mu$ M biotin-maleimide or biotin-iodoacetamide (Thermo Fisher Scientific, Rockford, IL) and incubated at 37 °C for 30 min. Biotin labeling was quenched with 50 mM DTT or gel loading buffer containing 10 mM DTT. Relative iNOS S-nitrosation levels were determined by immunoblotting for biotin labeling using the Vectastain ABC Kit (Vector Laboratories, Burlingame, CA) and SuperSignal West pico or femto maximum sensitivity substrate (Thermo Fisher Scientific). To ensure equal protein loading between samples, the blots were stained with Ponceau stain after imaging.

## RESULTS

**Nitrosation and Inactivation of iNOS during Enzymatic Turnover.** To gain insight into the physiological role of NOS S-nitrosation, we first determined if there was a direct temporal correlation between iNOS S-nitrosation and inactivation. While iNOS was previously shown to be S-nitrosated by exogenously added NO<sup>8</sup> and endogenously generated NO at the heme cofactor,<sup>30</sup> the time scale of auto-S-nitrosation was not investigated. Here, iNOS was rapidly S-nitrosated by NO generated during the catalytic reaction (Figure 1A), and the

level of iNOS auto-S-nitrosation peaked at ~30 min and did not increase at 60 min. S-Nitrosation levels were determined

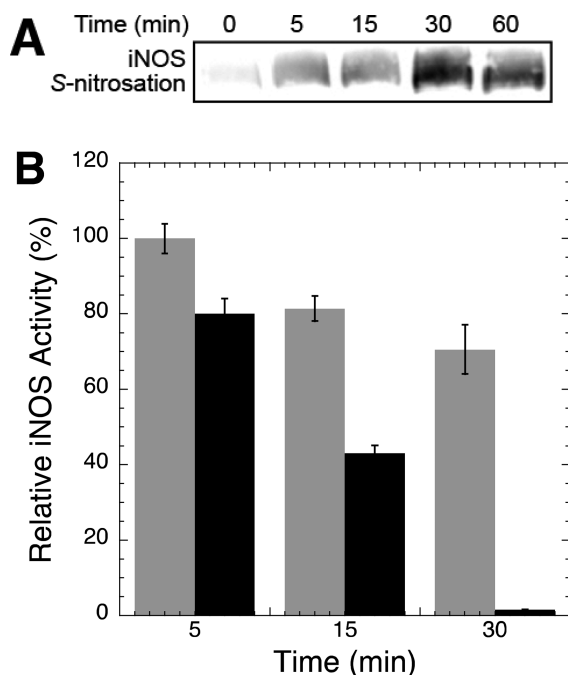


**Figure 1.** iNOS S-nitrosation and inactivation during enzymatic turnover. (A) iNOS S-nitrosation during enzymatic turnover. Each reaction mixture contained 4  $\mu$ M iNOS, 5 mM Arg, 2 mM NADPH, 50 mM NaCl, and 50 mM HEPES (pH 7.5). iNOS activity was initiated by addition of NADPH, and 100  $\mu$ L aliquots were taken at the indicated time points and quenched with an equal volume of 250 mM HEPES (pH 7.4) containing 2 mM EDTA, 0.2 mM neocuproine, 60 mM *N*-ethylmaleimide, and 10% SDS. Relative levels of iNOS S-nitrosation were determined by the biotin switch method (see Experimental Procedures). (B) iNOS inactivation during enzymatic turnover. Two separate reaction mixtures contained 90 nM iNOS, 15 mM Arg, 150 mM NaCl, and 100 mM HEPES (pH 7.5). In one mixture, iNOS activity was initiated at time zero by addition of NADPH (600  $\mu$ M) (black bars); in the other, NADPH was only added immediately prior to rate determination (gray bars). At the given time points, 100  $\mu$ L aliquots of each mixture were added to 200  $\mu$ L of 45  $\mu$ M MbO<sub>2</sub> in 100 mM HEPES (pH 7.5), yielding final concentrations of 30 nM iNOS, 5 mM Arg, 50 mM NaCl, 30  $\mu$ M MbO<sub>2</sub>, and 100 mM HEPES (pH 7.5).

using the biotin switch assay,<sup>11</sup> which selectively and covalently labels sites of S-nitrosation with biotin for detection by immunoblotting.

Exogenous addition of NO was previously shown to inactivate NOS *in vitro*.<sup>8,31–33</sup> This inactivation correlated with iNOS dimer dissociation due to S-nitrosation of the Zn<sup>2+</sup>-tetrathiolate.<sup>8</sup> However, the time scale of inactivation by endogenously generated NO at the heme cofactor had not been investigated. To determine the time scale of iNOS auto-inactivation, iNOS-catalyzed NO formation (and thus auto-S-nitrosation) was initiated by addition of both Arg and NADPH at time zero, and the remaining iNOS activity at 5, 15, and 30 min was determined using the increase in absorbance at 401 nm upon reaction of NO with oxymyoglobin (MbO<sub>2</sub>) to form nitrate and metmyoglobin (metMb). Indeed, iNOS-catalyzed NO formation resulted in the rapid loss of NOS activity (Figure 1B, black bars) that correlated with an increase in the level of iNOS auto-S-nitrosation (Figure 1A). A similar rapid decline in

nNOS activity was previously observed with near complete inactivation after 30–90 min.<sup>34,35</sup> To ensure the observed iNOS inactivation was a direct result of NOS activity and not general protein instability at room temperature, only Arg was added at time zero and NADPH was not added until immediately prior to assaying the rate at each time point. A relatively modest loss of iNOS activity was observed under these conditions (Figure 1B, gray bars), indicating that iNOS auto-inactivation was a direct result of NOS activity and auto-S-nitrosation.

Importantly, addition of superoxide dismutase (SOD) (50 units) and catalase (50 units) failed to protect iNOS from inactivation and instead resulted in a slight (~15%) increase in the level of iNOS inactivation (data not shown). A similar slight increase in inactivation rate was previously observed upon addition of SOD to iNOS<sup>36</sup> and eNOS<sup>31</sup> activity assays. This result indicated that iNOS autoinactivation was not due to generation of reactive oxygen species from uncoupling of the iNOS reductase and oxidase domains.

**Kinetic Model of iNOS Autoinactivation.** The observation that iNOS autoinactivation directly correlated with an increase in the level of iNOS auto-S-nitrosation led us to develop a kinetic model for iNOS inactivation by S-nitrosation

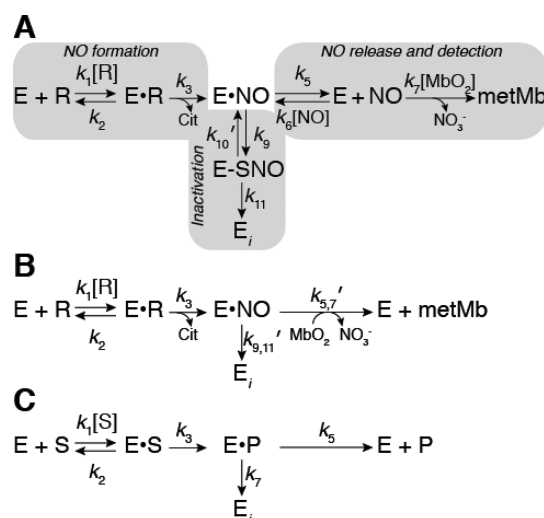


**Figure 2.** Kinetic model of iNOS inactivation. (A) Complete kinetic model of iNOS autoinactivation by S-nitrosation and dimer dissociation where the kinetic readout is reaction of NO with MbO<sub>2</sub>. Gray boxes indicate the NO formation, inactivation, and NO release–detection pathways. E represents the enzyme (i.e., iNOS), R arginine, E·R arginine bound within the iNOS active site, E·NO nitric oxide sequestered within iNOS but not necessarily bound to the heme iron, E·SNO iNOS S-nitrosated at the Zn<sup>2+</sup>-tetrathiolate cysteines, and E<sub>i</sub> inactivated iNOS. (B) Simplified kinetic model in which the inactivation and NO release–detection pathways are represented by net rate constants. (C) General kinetic model of a suicide substrate where S represents the substrate and P the product.

(Figure 2A). In this model, binding of Arg to iNOS ( $k_1$  and  $k_2$ ) is followed by irreversible formation of NO and citrulline ( $k_3$ ) (NO formation pathway). The NO formed at the heme cofactor is then released into solution ( $k_5$  and  $k_6$ ) where NO then reacts with MbO<sub>2</sub> to form nitrate and metMb ( $k_7$ ) (NO release–detection pathway). Alternatively, NO may react with the Zn<sup>2+</sup>-tetrathiolate resulting in S-nitrosation ( $k_9$ ) followed by dimer dissociation and inactivation ( $k_{11}$ ) (S-nitrosation–inactivation pathway).



Prior to dimer dissociation, S-nitrosation can be reversed ( $k_{10}'$ ) through addition of exogenous reductants (see below). Note that E-NO represents NO sequestered within iNOS such that the NO is inaccessible to MbO<sub>2</sub>, but not necessarily bound to the heme iron. Therefore,  $k_6$  represents the diffusion of NO into the iNOS protein environment, not NO binding to the heme iron. The kinetic model in Figure 2A can be further simplified by replacing the NO release–detection and inactivation pathways with net rate constants (Figure 2B):

$$k_{5,7}' = \frac{k_5 k_7 [\text{MbO}_2]}{k_5 + k_6 + k_7 [\text{MbO}_2]} \quad (1)$$

$$k_{9,11}' = \frac{k_9 k_{11}}{k_9 + k_{10}' + k_{11}} \quad (2)$$

The kinetic model in Figure 2B is identical to that of a suicide substrate (mechanism-based inhibitor) (Figure 2C). Therefore, using suicide substrate analysis,<sup>37–43</sup> plots of NO formation over time may be fit to eq 3:

$$[\text{NO}] = [\text{NO}]_\infty (1 - e^{-\lambda t}) \quad (3)$$

where  $[\text{NO}]_\infty$  is the total concentration of NO formed at infinite time and  $\lambda$  is the NOS inactivation rate. Equation 3 provided excellent fits to progress curves of iNOS-catalyzed NO formation obtained using the MbO<sub>2</sub> assay (Figure 3).

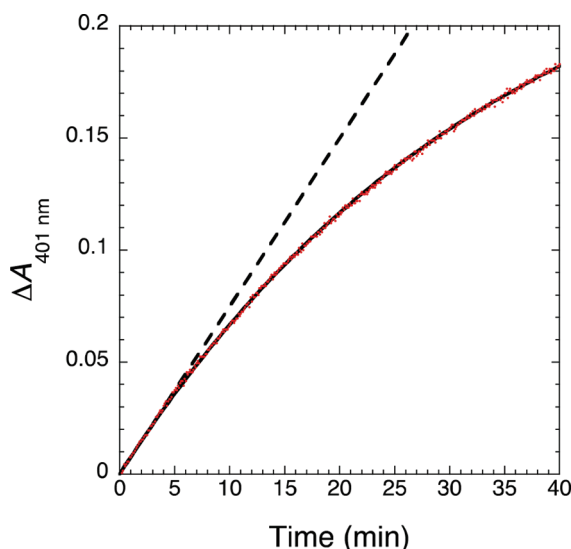


**Figure 3.** Progress curve of NO formation that exhibits inactivation over time. The reaction mixture contained 15 nM iNOS, 5 mM Arg, 200 μM NADPH, 50 mM NaCl, 4 μM MbO<sub>2</sub>, and 100 mM HEPES (pH 7.5) in a total volume of 300 μL in a 96-well microplate. NO formation was assessed by the increase in absorbance at 401 nm observed upon reaction of NO with MbO<sub>2</sub> to form metMb and nitrite. Data were fitted to eq 3, and the resulting fit is shown as a solid black line. The dashed line represents the linear fit to the first 5 min of the progress curve.

MbO<sub>2</sub> rapidly reacts with NO to form nitrate and metMb at a rate of  $3.4 \times 10^7 \text{ M}^{-1} \text{ s}^{-1}$ ,<sup>44</sup> which may be followed spectrally by a change in absorbance at 401, 540, or 581 nm. The time scale of inactivation in the MbO<sub>2</sub> assay (Figure 3) was slower than that of the assay without MbO<sub>2</sub> (Figure 1B), because MbO<sub>2</sub> reacts with

NO, further indicating that NO is the primary source of iNOS inactivation.

Using suicide substrate analysis,<sup>37–43</sup>  $[\text{NO}]_\infty$  and  $\lambda$  can be expressed in terms of the kinetic model rate constants:

$$\lambda = \frac{k_3 k_{9,11}'}{k_3 + k_{5,7}' + k_{9,11}'} \quad (4)$$

$$[\text{NO}]_\infty = r[\text{iNOS}] = \frac{k_{5,7}'}{k_{9,11}'} [\text{iNOS}] \quad (5)$$

where  $r$  is the partition ratio between the NO release–detection and S-nitrosation–inactivation pathways. This partition ratio can easily be determined for a given set of conditions via a plot of  $[\text{NO}]_\infty$  versus the initial iNOS concentration. If Arg is a suicide substrate, then this plot is predicted to give a straight line that intersects the origin with a slope equal to  $r$ . Indeed, fitting a plot of  $[\text{NO}]_\infty$  versus iNOS concentration at saturating substrate concentrations and 4 μM MbO<sub>2</sub> yielded a straight line that passed through the origin with a slope of  $106 \pm 2$  (Figure S1 of the Supporting Information). This indicated that ~100 molecules of NO were released into solution and reacted with MbO<sub>2</sub> for every one molecule of NO that led to S-nitrosation of the Zn<sup>2+</sup>-tetrathiolate. However, it should be noted that the  $[\text{NO}]_\infty$  value and therefore the  $r$  value greatly depend on the MbO<sub>2</sub> concentration utilized in the assay. This ability of MbO<sub>2</sub> to “trap” solution NO and alter the inactivation rate will be exploited below.

**Reductants Protect iNOS from S-Nitrosation and Inactivation.** Thiols like glutathione (GSH) and other reducing agents such as TCEP are capable of reducing nitrosothiols to free thiols. GSH and other thiol reducing agents were shown to prevent iNOS<sup>45,46</sup> and nNOS inactivation.<sup>35,47</sup> Therefore, the inactivation pathway of the kinetic model (Figure 2A) can be perturbed through addition of reducing agents. Indeed, both GSH (Figure 4A) and TCEP (Figure 4B) reduced the inactivation rate, though TCEP required a concentration approximately 2 orders of magnitude lower than that of GSH for a similar effect.

As only a finite concentration of S-nitrosated iNOS (E-SNO in Figure 2A) exists, we hypothesized that addition of a reducing agent would exhibit saturation kinetics and alter the rate of nitrosothiol reduction ( $k_{10}'$ ) through the following relationship:

$$k_{10}' = \frac{k_{10} [\text{reductant}]}{K_{m,\text{app}}^{\text{red}} + [\text{reductant}]} \quad (6)$$

where  $k_{10}$  is the maximal rate of nitrosothiol reduction,  $[\text{reductant}]$  is the GSH or TCEP concentration, and  $K_{m,\text{app}}^{\text{red}}$  is the apparent  $K_m$  of nitrosothiol reduction. Therefore, when no reductant is added to the assay mixture,  $k_{10}' = 0$  and nitrosothiol formation is irreversible and committed to enzyme inactivation. Plots of  $[\text{NO}]_\infty$  versus  $[\text{reductant}]$  yielded excellent fits to the relationship between  $[\text{NO}]_\infty$  and  $[\text{reductant}]$  shown in eq 7 derived from eqs 2, 5, and 6 (Figure 4C).

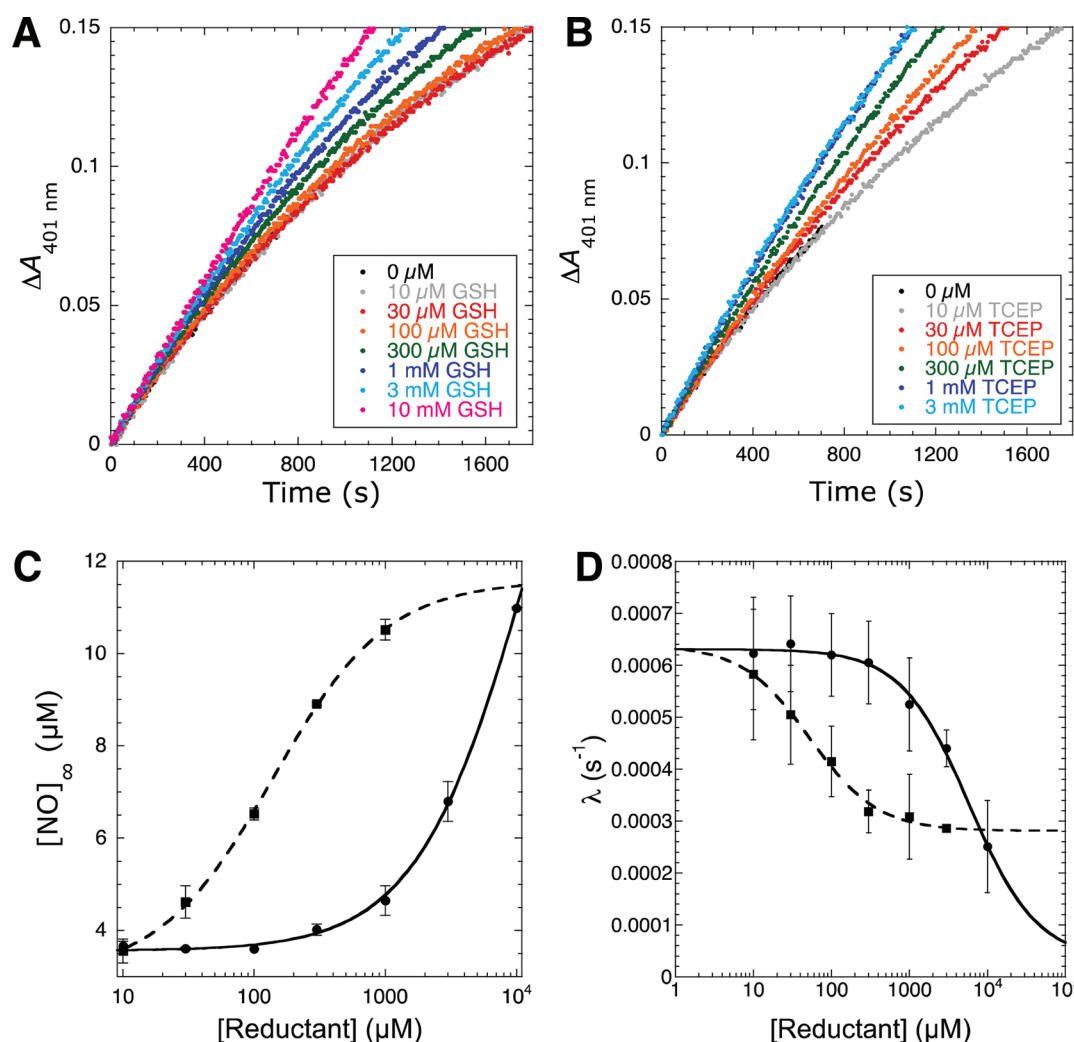


**Figure 4.** Protection of iNOS inactivation by reductants. Progress curves of iNOS-catalyzed NO formation in the presence of increasing concentrations of (A) GSH and (B) TCEP. Individual reaction mixtures contained 15 nM iNOS, 5 mM Arg, 200  $\mu$ M NADPH, 50 mM NaCl, 4  $\mu$ M MbO<sub>2</sub>, 100 mM HEPES (pH 7.5), and varying concentrations of either GSH or TCEP in total volumes of 300  $\mu$ L in a 96-well microplate. NO formation was measured via the change in absorbance at 401 nm upon reaction of MbO<sub>2</sub> with NO. (C) Plot of [NO]<sub>∞</sub> vs GSH (●, solid line) or TCEP (■, dashed line) concentration. Data were fit using eqs 2, 5, and 6. (D) Plot of inactivation rate ( $\lambda$ ) vs GSH (●, solid line) or TCEP (■, dashed line) concentration. Data were fit using eqs 2, 4, and 6.

$$[\text{NO}]_{\infty} = k_{5,7}'[\text{iNOS}] \left( \frac{1}{k_9} + \frac{1}{k_{11}} \right) + \left( \frac{k_{5,7}'k_{10}[\text{iNOS}]}{k_9k_{11}} \right) \left( \frac{[\text{reductant}]}{K_{m,\text{app}}^{\text{red}} + [\text{reductant}]} \right) \quad (7)$$

Similarly, plots of  $\lambda$  versus [reductant] also yielded excellent fits to the relationship derived from eqs 2, 4, and 6 (Figure 4D). These experiments and those described below allowed estimation of values for the various kinetic constants in the kinetic model. In general, data plots were fit using nonlinear regression in Kaleidagraph (Synergy Software, Reading, PA), and the resulting kinetic constants are listed in Table 1.

If iNOS auto-S-nitrosation is the main source of auto-inactivation, protection from inactivation by reductants should correlate with a decrease in the level of S-nitrosation. Indeed,

using the biotin switch assay, a decrease in the level of iNOS S-nitrosation was observed with increasing concentrations of both GSH and TCEP (Figure 5). In particular, a concentration-dependent decrease in the level of iNOS auto-S-nitrosation was observed at >1 mM GSH and >30  $\mu$ M TCEP. Importantly, the effect of both reductants on iNOS S-nitrosation correlated well with the observed decrease in inactivation rate at varying reductant concentrations (Figure 4D).

The kinetic model described above (Figure 2) indicates iNOS is only inactivated upon dimer dissociation ( $k_{11}$ ) following S-nitrosation ( $k_9$ ). If this model is correct, then added reductants ( $k_{10}'$ ) should protect S-nitrosated iNOS (E-SNO) from inactivation but not recover activity from inactivated iNOS ( $E_i$ ) as  $k_{11}$  is irreversible. To determine if the activity of inactivated iNOS could be recovered by addition of reductant, iNOS was fully inactivated as in Figure 1B at which point 3 mM GSH or 1 mM TCEP was added and the resulting iNOS activity was assayed. iNOS activity was not recovered by this method (data not shown), indicating that iNOS inactivation is irreversible. This result was consistent with

**Table 1. Rate Constants Derived from the Kinetic Model of Inactivation**

rate constant	kinetic model step	reductant titration	varying MbO <sub>2</sub>
$k_3$ (s <sup>-1</sup> )	NO formation	NA	~2.2 <sup>a</sup>
$k_5$ (s <sup>-1</sup> )	diffusion of NO from NOS	NA	16.1 ± 5.6 <sup>b</sup>
$k_6$ [NO] (s <sup>-1</sup> )	diffusion of NO into NOS	NA	(1.6 ± 0.6) × 10 <sup>3b</sup>
$k_7$ (M <sup>-1</sup> s <sup>-1</sup> )	reaction of MbO <sub>2</sub> with NO	3.4 × 10 <sup>7c</sup>	3.4 × 10 <sup>7c</sup>
$(k_9 k_{11})/(k_9 + k_{11})$ (s <sup>-1</sup> )	inactivation pathway without reductant	(6.7 ± 0.2) × 10 <sup>-4d</sup>	(7.4 ± 2.5) × 10 <sup>-4b</sup>
$(k_9 k_{11})/(k_9 + k_{10} + k_{11})$ (s <sup>-1</sup> )	inactivation pathway with saturating reductant	(1.1 ± 0.1) × 10 <sup>-4d</sup>	NA
$k_{10}^{\text{GSH}}/k_{10}^{\text{TCEP}}$	S-nitrosothiol reduction	2.0 ± 0.2 <sup>d</sup>	NA
$K_{m,\text{app}}^{\text{GSH}}$ (μM)		(1.3 ± 0.2) × 10 <sup>4d</sup>	NA
$K_{m,\text{app}}^{\text{TCEP}}$ (μM)		(1.4 ± 0.1) × 10 <sup>2d</sup>	NA

<sup>a</sup>The rate was approximated from the single-turnover rate of formation of NHA from arginine, the single-turnover rate of NO, the rate of formation of citrulline from NHA, and the rate of release of NO from iNOS ferric heme.<sup>50–54</sup> <sup>b</sup>Rate determined from the fit in Figure 7A. <sup>c</sup>Rate from ref 44. <sup>d</sup>Rate determined from the fit in Figure 5C.

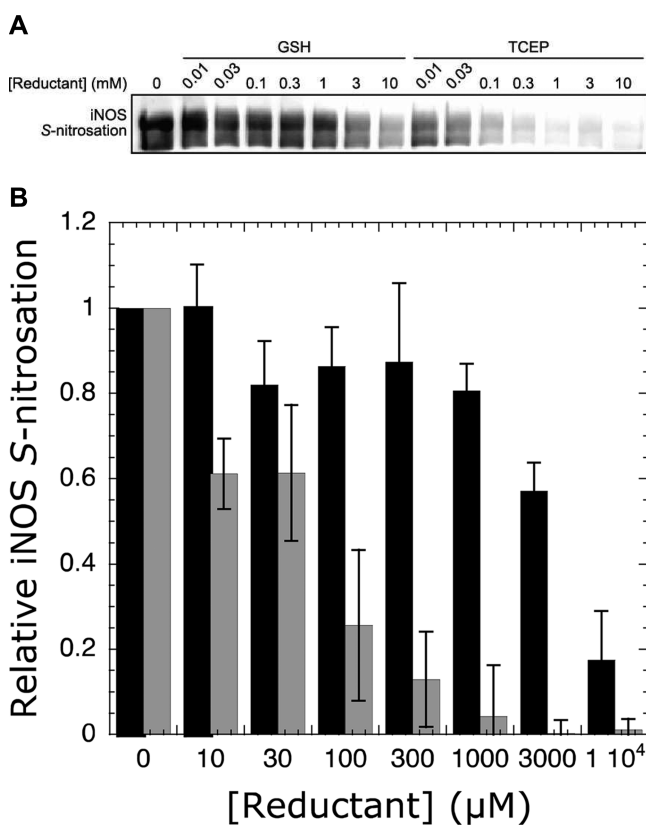


**Figure 5. Protection of iNOS auto-S-nitrosation by reductants.** (A) The anti-biotin blot shows a dose-dependent decrease in the level of iNOS S-nitrosation upon addition of GSH and TCEP. (B) Quantitation of anti-biotin blots with increasing concentrations of GSH (black bars) and TCEP (gray bars). Levels of iNOS S-nitrosation were normalized to the level observed with no added reductant. Error bars represent the standard deviation from the mean. Each reaction mixture contained 2 μM iNOS, 5 mM Arg, 2 mM NADPH, 50 mM NaCl, and varying concentrations of either GSH or TCEP in HEN buffer [250 mM HEPES, 2 mM EDTA, and 0.2 mM neocuproine (pH 7.5)] in a total volume of 100 μL. iNOS activity was initiated by addition of NADPH and quenched after 20 min in HEN buffer with 60 mM N-ethylmaleimide and 10% SDS. Relative levels of iNOS S-nitrosation were determined by the biotin switch method (see Experimental Procedures).

a previous study in which GSH was added to fully inactivated nNOS and no recovery of nNOS activity was observed.<sup>35</sup> Therefore,  $k_{11}$  is a necessary irreversible rate constant as part of the kinetic model (Figure 2A). The inability to

recover inactivated iNOS is also consistent with the hypothesis that dimer dissociation following S-nitrosation and Zn<sup>2+</sup> loss, not S-nitrosation or Zn<sup>2+</sup> loss itself, is responsible for inactivation.

**The iNOS Inactivation Rate Depends on the Rate of NO Formation.** Further insight into the kinetic model was obtained through perturbation of the NO formation pathway (Figure 2A). This was done by utilization of subsaturating Arg concentrations. When Arg is not saturating, [NO]<sub>∞</sub> is governed by eq 8:<sup>37</sup>

$$[\text{NO}]_{\infty} = \frac{k_{5,7}'[\text{iNOS}][\text{Arg}]}{k_{9,11}'\left([\text{Arg}] + \frac{k_3 + k_{5,7}' + k_{9,11}'}{k_3}K_m\right)} = \frac{k_{5,7}'[\text{iNOS}][\text{Arg}]}{k_{9,11}'([\text{Arg}] + K_{m,\text{app}})} \quad (8)$$

where  $K_m$  is the Michaelis constant for Arg previously determined to be 8.6 μM.<sup>48</sup> Note that when Arg is saturating eq 9 reduces to eq 5. Also, note that the apparent  $K_m$  value for Arg ( $K_{m,\text{app}}$ ) is larger than the actual  $K_m$  value by a factor of  $(k_3 + k_{5,7}' + k_{9,11}')/k_3$ . Progress curves at varying Arg concentrations from 6.25 to 100 μM were fitted to eq 3 to determine [NO]<sub>∞</sub>, and then plots of [NO]<sub>∞</sub> versus Arg concentration (Figure S3 of the Supporting Information) were fitted to eq 9 by nonlinear regression using Kaleidagraph (Synergy Software) to obtain the  $k_{5,7}'/k_{9,11}'$  ratio and apparent  $K_m$  value. Using 8 μM MbO<sub>2</sub>, an apparent  $K_m$  value of 42 ± 2 μM and a  $k_{5,7}'/k_{9,11}'$  ratio of 690 ± 20 were determined. Alternatively, eq 8 may be rearranged to give eq 9:

$$\frac{[\text{iNOS}]}{[\text{NO}]_{\infty}} = \frac{k_{9,11}'}{k_{5,7}'} + \frac{k_{9,11}'K_{m,\text{app}}}{k_{5,7}'[\text{Arg}]} \quad (9)$$

Therefore, the plot of [iNOS]/[NO]<sub>∞</sub> versus 1/[Arg] was predicted to yield a straight line with an ordinate intercept of  $k_{9,11}'/k_{5,7}'$  and a slope of  $(k_{9,11}'K_m)/k_{5,7}'$ . Indeed, the plot of [iNOS]/[NO]<sub>∞</sub> versus 1/[Arg] yielded a straight line (inset of Figure S3 of the Supporting Information) with a  $k_{9,11}'/k_{5,7}'$  value of 0.0011 ± 0.0002 and a  $(k_{9,11}'K_m)/k_{5,7}'$  value of 0.069 ± 0.002. The positive slope observed highlighted the difference between Arg and a classical suicide substrate as the plot of [E]/[P]<sub>∞</sub> versus 1/[S] for a classical suicide substrate would yield a horizontal line because [P]<sub>∞</sub> is independent of substrate concentration. A classical suicide substrate binds the enzyme and then reacts within the active site in a manner that prevents

subsequent substrate binding and turnover. In contrast, NO inactivates iNOS at a site distal to the active site (i.e., the Zn<sup>2+</sup>-tetrathiolate). Thus, Arg binding and turnover proceed until iNOS S-nitrosation, dimer dissociation, and enzyme inactivation occur, and [NO]<sub>∞</sub> depends on the relative flux between the NO formation and inactivation pathways at subsaturating Arg concentrations.

**NO Traps Decrease the iNOS Inactivation Rate.** Finally, varying concentrations of solution NO traps were used to perturb the NO release–detection pathway (Figure 2A). Previously, oxyhemoglobin (HbO<sub>2</sub>) was utilized as a solution NO trap to protect nNOS<sup>32,33</sup> and eNOS<sup>31,49</sup> from autoinactivation in activity assays. Here, in place of hemoglobin, horse heart myoglobin was utilized because it lacks cysteine residues and thus avoids potential assay artifacts due to reaction of NO or nitrosothiols with cysteines. Using a saturating level of Arg, the inactivation rate was determined at varying concentrations of MbO<sub>2</sub> from 4 to 160 μM. The resulting plot of λ versus MbO<sub>2</sub> concentration exhibited a dependence on the amount of trap at low MbO<sub>2</sub> concentrations but was independent at high MbO<sub>2</sub> concentrations. The trap-dependent portion of the plot is likely due to competition between MbO<sub>2</sub> and the Zn<sup>2+</sup>-tetrathiolate for reaction with NO in solution; the trap-independent portion likely indicates that a portion of NO reacts with the Zn<sup>2+</sup>-tetrathiolate without first being released into solution (see Discussion). This concentration-dependent trap result was predicted from the kinetic model, and plots of λ versus MbO<sub>2</sub> concentration yielded excellent fits to the relationship between λ and MbO<sub>2</sub> concentration derived from eqs 1 and 4 (Figure 6A). To simplify the determination of individual kinetic constants in the kinetic model, we fit the plot of 1/λ versus MbO<sub>2</sub> concentration (Figure 6A, inset) to eq 10 using Kaleidagraph (Synergy Software).

$$\frac{1}{\lambda} = \frac{1}{k_3} + \frac{1}{k_{9,11'}} + \left( \frac{k_5}{k_3 k_{9,11'}} \right) \left( \frac{k_7 [\text{MbO}_2]}{k_5 + k_6 [\text{NO}] + k_7 [\text{MbO}_2]} \right) \quad (10)$$

Because  $k_3$  could be estimated from published single-turnover rates of heme reduction,<sup>50</sup> Arg oxidation,<sup>51</sup> and NO formation from *N*-hydroxyarginine,<sup>52–54</sup> the plot of 1/λ versus [MbO<sub>2</sub>] allowed direct determination of  $k_5$ ,  $k_6$ [NO], and  $k_{9,11'}$  (Table 1).

To ensure that the effect of MbO<sub>2</sub> on the inactivation rate was not due to some property of MbO<sub>2</sub> other than the ability to trap solution NO, the ability of apomyoglobin and metmyoglobin (metMb) to protect iNOS from inactivation was tested. The addition of increasing concentrations of apomyoglobin or metMb to 5 μM MbO<sub>2</sub><sup>a</sup> failed to decrease the inactivation rate (data not shown). Similarly, addition of metHb had no effect on nNOS<sup>33</sup> or eNOS<sup>31</sup> inactivation in previous studies. In addition, inhibition of iNOS by the nitrate generated from the reaction of NO with MbO<sub>2</sub> could not account for the decrease in inactivation rate, as nitrate concentrations of ≤ 1 mM did not alter iNOS activity (data not shown). The lack of iNOS inhibition by nitrate was in line with previous reports examining nitrite and nitrate inhibition of nNOS.<sup>33,34</sup> Taken together, these observations indicate that the ability of increasing MbO<sub>2</sub> concentrations to decrease the inactivation rate was solely due to an improved ability to trap solution NO.

To assess whether the trap-independent inactivation rate observed at high MbO<sub>2</sub> concentrations was due to a thiol-

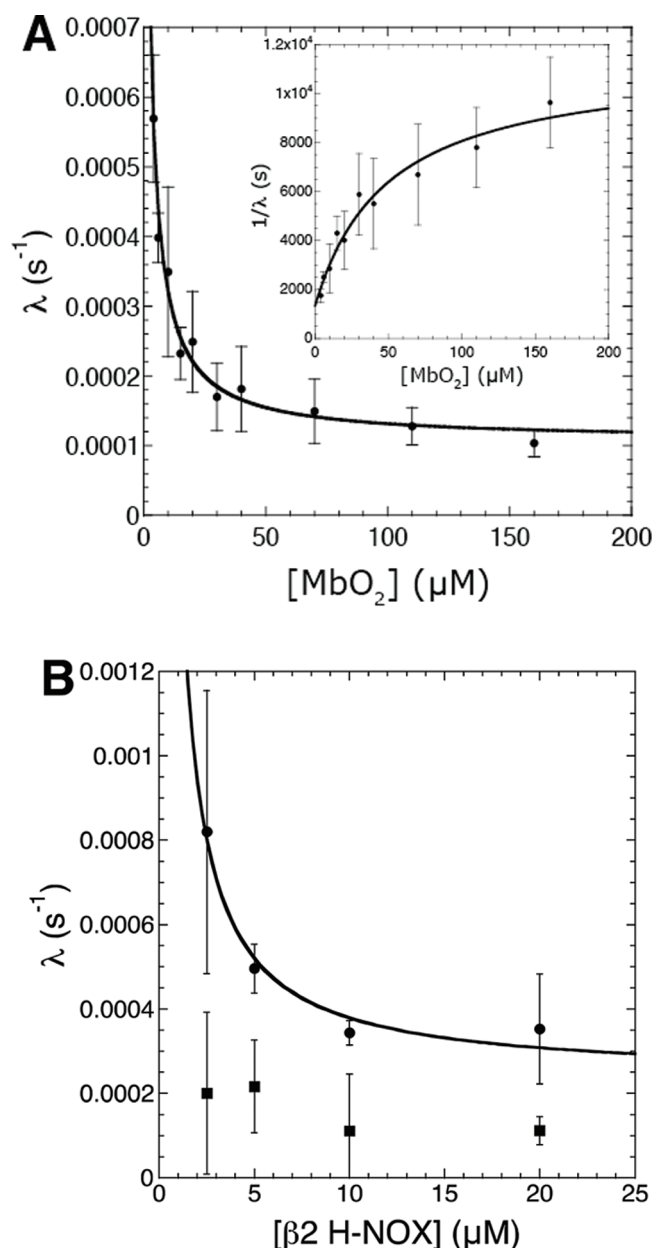


**Figure 6.** Plots of iNOS inactivation rate (λ) vs (A) MbO<sub>2</sub> concentration and (B) β2 H-NOX concentration. Individual reaction mixtures contained 15 nM iNOS, 5 mM Arg, 200 μM NADPH, 50 mM NaCl, 100 mM HEPES (pH 7.5), and varying concentrations of either MbO<sub>2</sub> or β2 H-NOX in total volumes of 300 μL in a 96-well microplate. NO formation was measured as described in Experimental Procedures. The resulting progress curves were fit to eq 3 to determine the inactivation rate (λ). The plots of inactivation rate (λ) vs NO trap concentration were fit using eqs 1 and 4. The inset in panel A was fit to eq 8.

dependent process (i.e., S-nitrosation) or other potential, independent inactivation processes, the concentration of NO traps were varied in the presence of 10 mM GSH. If trap-dependent and trap-independent inactivation were both a result of iNOS S-nitrosation, then addition of GSH would result in a horizontal line lying below the trap-independent inactivation rate in the plot of λ versus MbO<sub>2</sub> concentration. However, 10 mM GSH interfered with the MbO<sub>2</sub> assay at high MbO<sub>2</sub> concentrations.<sup>b</sup> Therefore, an alternative method for trapping and detecting NO without generating a ferric heme species was



sought. The heme domain (residues 1–217) of the  $\beta 2$  subunit of soluble guanylate cyclase ( $\beta 2$  H-NOX) is ideal in this respect as it is a native NO receptor, does not bind oxygen, is stable to oxidation, and binds NO with a characteristic spectral shift (Soret  $\lambda_{\text{max}}$  from 433 to 399 nm).<sup>24</sup> Therefore, the  $\beta 2$  H-NOX concentration was varied in a fashion similar to that used for MbO<sub>2</sub>, and inactivation rates were determined in the presence and absence of 10 mM GSH. Plots of  $\lambda$  versus  $\beta 2$  H-NOX concentration were similar to those using MbO<sub>2</sub> (Figure 6B) with one important distinction: the concentration of  $\beta 2$  H-NOX necessary to reach the trap independence was lower than with MbO<sub>2</sub>.<sup>c</sup> This correlates with the more rapid binding of NO to  $\beta 2$  H-NOX ( $>1.4 \times 10^8 \text{ M}^{-1} \text{ s}^{-1}$ ) compared to the reaction of NO with MbO<sub>2</sub> ( $3.4 \times 10^7 \text{ M}^{-1} \text{ s}^{-1}$ )<sup>44,55</sup> and further indicates that the observed decreases in inactivation rate were due to trapping solution NO. As hypothesized above, addition of 10 mM GSH resulted in constant inactivation rates over the entire range of  $\beta 2$  H-NOX concentrations, with an inactivation rate below the trap-independent inactivation rate (Figure 6B). This indicated the trap-dependent and trap-independent inactivations are both thiol-dependent processes (e.g., S-nitrosation). However, the inactivation rate with GSH was not zero because 10 mM GSH is not saturating for nitrosothiol reduction [the apparent  $K_m$  value for GSH is 13 mM (Table 1)], binding of NO to  $\beta 2$  H-NOX is reversible, and other minor processes besides S-nitrosation likely also result in inactivation (e.g., protein instability). Therefore, our data are consistent with both trap-dependent and trap-independent iNOS autoinactivation resulting from Zn<sup>2+</sup>-tetrathiolate S-nitrosation.

## DISCUSSION

**Kinetic Model of iNOS Autoinactivation.** Exposure of NOS to NO lowers the activity of NOS both in vitro<sup>8,10,31–33</sup> and in cells.<sup>31,56–58</sup> NO is also capable of S-nitrosating the NOS Zn<sup>2+</sup>-tetrathiolate,<sup>7–11,30,59</sup> which (at least for iNOS) results in the loss of zinc followed by irreversible dimer dissociation and inactivation.<sup>7,8</sup> Here, we present a detailed kinetic model of NOS S-nitrosation and inactivation by treating arginine as a suicide substrate (Figure 2). This kinetic model has allowed for the direct and quantitative determination of the inactivation rate ( $\lambda$ ), the NO concentration formed at infinite time ( $[\text{NO}]_{\infty}$ ), and the partition ratio between NO release and the NOS S-nitrosation–inactivation process. As discussed below, perturbation of this kinetic model by variation of the concentration of NO traps and reductants provided insight into the role of NOS S-nitrosation in NOS autoinactivation, the mechanism of NOS S-nitrosation, and the potential role of NOS S-nitrosation in the initial formation of nitrosothiols such as GSNO.

**S-Nitrosation and iNOS Autoinactivation.** The majority of the evidence previously reported and expanded upon here points to S-nitrosation of the Zn<sup>2+</sup>-tetrathiolate as being the primary mechanism of NOS autoinactivation, although some alternative mechanisms have been described, including modification of the pterin cofactor (see the Supporting Information). The time scale of iNOS S-nitrosation (Figure 1A) correlated exactly with the observed loss of iNOS activity (Figure 1B). Furthermore, the ability of reducing agents (i.e., GSH and TCEP) to protect iNOS from autoinactivation (Figure 4) also directly correlated with a decrease in iNOS S-nitrosation (Figure 5). Previous studies showed that treatment of activated macrophages with GSNO or S-nitroso-N-acetyl-penicillamine (SNAP) inactivated iNOS in a concentration-dependent

manner, consistent with inactivation occurring through trans-nitrosation of the Zn<sup>2+</sup>-tetrathiolate.<sup>56</sup> Addition of SNAP also inhibited nNOS activity in cytosolic extracts from rat brain.<sup>56</sup> Furthermore, SNAP inhibition of nNOS was irreversible, which was consistent with nNOS dimer dissociation following S-nitrosation of the Zn<sup>2+</sup>-tetrathiolate<sup>56</sup> being the cause of inactivation.

**Mechanism of iNOS S-Nitrosation.** Having determined that iNOS S-nitrosation is the primary mechanism of iNOS autoinactivation, we sought insight into the mechanism of iNOS S-nitrosation. As mentioned above, S-nitrosation is not a simple addition of NO to thiols; the conversion of a thiol to a nitrosothiol involves a one-electron oxidation. There are two main mechanisms of S-nitrosation.<sup>60</sup> One is an aerobic mechanism (with O<sub>2</sub> as the oxidant, forming N<sub>2</sub>O<sub>3</sub> as the nitrosating agent) in which N<sub>2</sub>O<sub>3</sub> reacts with free thiols to form nitrosothiols at a rate of  $\sim 6.6 \times 10^7 \text{ M}^{-1} \text{ s}^{-1}$ .<sup>61</sup> Alternately, thiyl radicals of cellular thiols (e.g., GS<sup>•</sup>) can react with NO at a rate of  $\sim 3 \times 10^9 \text{ M}^{-1} \text{ s}^{-1}$ <sup>62</sup> to produce nitrosothiols. For iNOS, O<sub>2</sub> appears to be the oxidant for S-nitrosation, as treatment of iNOS with exogenous NO under anaerobic conditions yielded no S-nitrosation.<sup>8</sup> This requirement of O<sub>2</sub> for S-nitrosation is consistent with N<sub>2</sub>O<sub>3</sub> as the nitrosating agent for iNOS, but other aerobic oxidation mechanisms cannot be ruled out.

In cells, NO concentrations are in the nanomolar to low micromolar range, but the concentrations of species that bind, react with, and destroy NO are several orders of magnitude higher (heme proteins, reductants, oxygen, superoxide, iron–sulfur clusters, etc.). Lim et al. estimated using a kinetic model that, at NO concentrations representative of an inflammatory response (1  $\mu\text{M}$ ), solution N<sub>2</sub>O<sub>3</sub> concentrations are limited to the femtomolar range.<sup>63</sup> These low estimated N<sub>2</sub>O<sub>3</sub> concentrations were primarily due to the ability of GSH to scavenge NO and react with N<sub>2</sub>O<sub>3</sub>. Regardless of the exact mechanism of Zn<sup>2+</sup>-tetrathiolate S-nitrosation, the results presented here are consistent with iNOS forming the relevant nitrosating agent sequestered within the protein environment, thus avoiding reactions with GSH and other species that destroy NO.

The trap-dependent and trap-independent components observed upon fitting our kinetic model (Figure 2) at varying trap concentrations (Figure 6) support the hypothesis that NO sequestered within the protein environment is responsible for iNOS S-nitrosation. The trap-independent component suggests that NO generated at the heme cofactor can S-nitrosate iNOS without being released into solution. Importantly, assays varying the  $\beta 2$  H-NOX concentration in the presence of 10 mM GSH (Figure 6B) showed that the majority of the trap-independent component was thiol-dependent consistent with inactivation due to S-nitrosation. Interestingly, examination of iNOS crystal structures revealed a tunnel between the two heme-binding sites that passes directly by the Zn<sup>2+</sup>-tetrathiolate (Figure 7A). Similar tunnels were also found in eNOS [Protein Data Bank (PDB) entry 1DOC] and nNOS (PDB entry 1OM4) crystal structures. It is important to note that the Zn<sup>2+</sup>-tetrathiolate is positioned directly between this tunnel and the solvent-exposed surface of NOS. Therefore, S-nitrosation of the Zn<sup>2+</sup>-tetrathiolate might occur via this conduit tunnel, resulting in surface-exposed nitrosothiols that may participate in downstream transnitrosation reactions with GSH or other proteins. The hypothesis that the NOS nitrosothiols are surface-exposed is supported by the ability of both GSH and TCEP (which is structurally unrelated to GSH) to efficiently reduce the level of



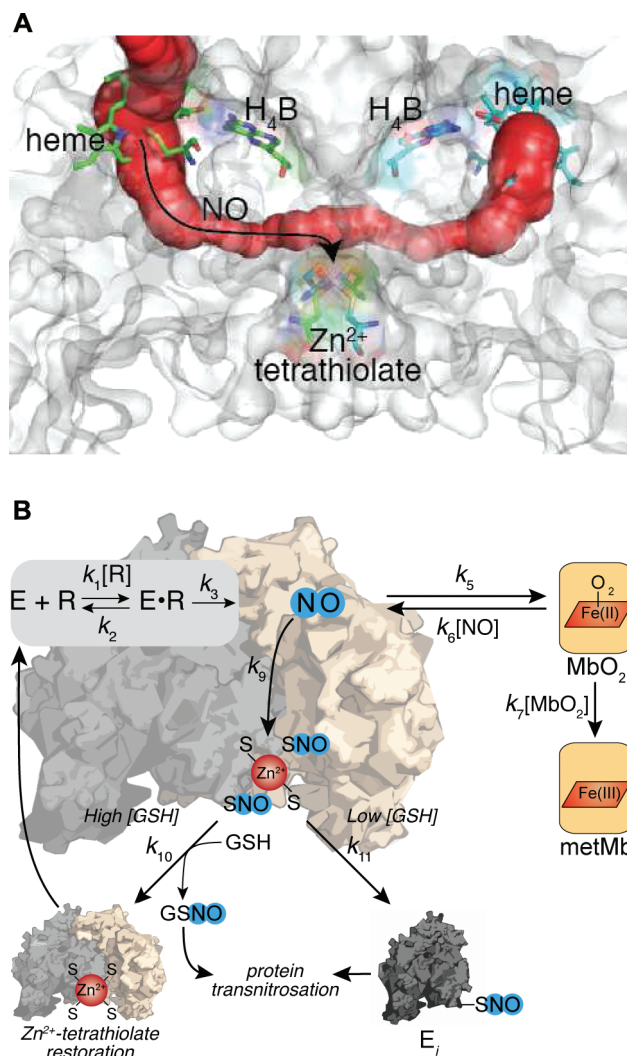


**Figure 7.** (A) Potential tunnel for diffusion of NO from the heme to the Zn<sup>2+</sup>-tetrathiolate within iNOS. The tunnel within a structure of the iNOS heme domain (PDB entry 1DWV)<sup>85</sup> was generated using CAVER.<sup>86</sup> (B) Summary model of iNOS autoinactivation through S-nitrosation of the Zn<sup>2+</sup>-tetrathiolate and protection from inactivation by reductants. The illustrated scheme is superimposed on the kinetic model that was developed by treating the substrate arginine as a mechanism-based inhibitor. Rescue by cellular reductants (GSH) is also shown as well as trapping of released NO by MbO<sub>2</sub>.

iNOS S-nitrosation (Figure 5). This use of a protein tunnel represents a novel mechanism for directing NO reactivity.

The trap-dependent component suggests that a component of iNOS inactivation involves competition of the Zn<sup>2+</sup>-tetrathiolate and MbO<sub>2</sub> for solution NO. In the kinetic model (Figure 2), the rate of NOS competition for solution NO is represented by the rate constant  $k_6[\text{NO}]$  (Table 1). From the rate of rebinding of NO to the heme upon photodissociation, Slama-Schwok et al. estimated that approximately four non-heme-bound NO molecules can reside within the eNOS oxidase domain.<sup>64</sup> If we estimate that, like eNOS, iNOS also possesses four non-heme NO binding sites per monomer in addition to the heme binding site, then the steady state NO concentration can be estimated to be ~75 nM as 15 nM iNOS was utilized in our assays. Using this analysis, the estimated bimolecular rate of sequestration of NO by iNOS ( $k_6$  in Figure 2)

is  $\sim 10^{10} \text{ M}^{-1} \text{ s}^{-1}$ . As N<sub>2</sub>O<sub>3</sub> nitrosates GSH at a rate of  $6.6 \times 10^7 \text{ M}^{-1} \text{ s}^{-1}$ ,<sup>61</sup> either the iNOS Zn<sup>2+</sup>-tetrathiolate is more than 2 orders of magnitude more reactive toward N<sub>2</sub>O<sub>3</sub> than GSH, N<sub>2</sub>O<sub>3</sub> is not the relevant nitrosating agent, or all S-nitrosation occurs through the tunnel (Figure 7A). In the last case, the trap-dependent component would result from competition of NO released into solution between reaction with MbO<sub>2</sub> and diffusion back into iNOS (Figure 7B). Furthermore, rates of  $\sim 10^{10} \text{ M}^{-1} \text{ s}^{-1}$  are within reason for diffusion of gases into protein environments.<sup>65</sup>

Several other lines of evidence are consistent with the ability of NOS to sequester NO and generate nitrosating agents within the protein environment. First, non-heme NO binding sites have been observed in NOS crystal structures.<sup>66</sup> Second, HbO<sub>2</sub> was found to be much more efficient in protecting iNOS from inactivation by exogenously added NO compared to generated NO at the active site during turnover,<sup>36</sup> suggesting that NO does not dissociate from iNOS prior to S-nitrosation of the Zn<sup>2+</sup>-tetrathiolate. Finally, the interior of NOS is largely hydrophobic, and the S-nitrosation of proteins is accelerated in a hydrophobic environment.<sup>67</sup> Therefore, a high local concentration of NO and oxygen sequestered within NOS may accelerate the formation of the nitrosating agent (e.g., N<sub>2</sub>O<sub>3</sub>) involved in NOS S-nitrosation.

**GSH Protection of iNOS from S-Nitrosation and Inactivation.** In assays without added reductant, iNOS is fully inactivated in ~30 min (Figure 1B). Millimolar GSH concentrations were sufficient to protect iNOS from S-nitrosation and inactivation, but significant iNOS S-nitrosation and inactivation was observed at micromolar GSH concentrations (Figures 5 and 6). Therefore, iNOS might only inactivate in vivo once GSH concentrations reach micromolar levels. In particular, the kinetic data presented here suggest that the rate of iNOS autoinactivation (i.e.,  $\lambda$ ) and the total concentration of NO synthesized (i.e.,  $[\text{NO}]_{\infty}$ ) are carefully controlled by the concentration of reduced cellular thiols (e.g., GSH). Additionally, proteins that may be direct targets of NOS transnitrosation (e.g., COX-2, caspase-3, or arginase 1) may protect NOS from autoinactivation. Intriguingly, iNOS is most responsive to low millimolar concentrations of GSH, which corresponds to the GSH concentration in normal cells (1–5 mM).<sup>17</sup> In cases where GSH levels drop from low millimolar to high micromolar concentrations (e.g., during endotoxemia<sup>68,69</sup> or ischemia/reperfusion<sup>70</sup> in hepatocytes or during macrophage activation<sup>71</sup>), significant iNOS inactivation would be predicted. Indeed, in activated macrophages, total glutathione concentrations (GSH and GSSG) decreased by 45% and the GSH:GSSG ratio decreased from 12:1 to 2:1 after 48 h. This decrease in GSH levels directly correlated with a decrease in NOS activity.<sup>71</sup> Depletion of cellular GSH levels through chemical means also led to a sharp decrease in iNOS activity in induced macrophages<sup>71,72</sup> or hepatocytes<sup>46,73</sup> and eNOS activity in endothelial cells.<sup>74–77</sup> Addition of GSH<sup>46,74</sup> or glutathione ethyl ester<sup>72,78</sup> concurrently with GSH-depleting small molecules resulted in protection from NOS inactivation. However, addition of GSH to induced macrophage cytosolic extracts failed to recover iNOS activity,<sup>72</sup> suggesting that GSH protects iNOS from inactivation in vivo but that GSH is incapable of recovering activity once iNOS is inactivated, an observation that mirrors the in vitro results reported here.

**Implications for NOS S-Nitrosation in the Physiological Generation of Nitrosothiols.** To gain insight into the physiological relevance of NOS S-nitrosation as an initial source

of nitrosothiols, we determined the partition ratio of NO release versus iNOS S-nitrosation/inactivation (Figure 2) at varying concentrations of NO traps (Figure 6). In vivo, this partition ratio likely resembles the trap-independent component in Figure 6 as the concentrations of species that bind, react with, and destroy NO are high compared to iNOS concentrations. Therefore, NO release is likely irreversible in vivo, and the partition ratio is represented by  $k_5/k_{9,11}$ , which is  $\sim 22000$  (Table 1). The  $k_{9,11}$  value used in this calculation was the higher value without added reductant because GSH reversal of iNOS S-nitrosation also results in the formation of a nitrosothiol, GSNO. Importantly, the half-life of NO in vivo is on the order of 2 ms to 2 s,<sup>79,80</sup> and the half-lives of nitrosothiols in plasma are  $\sim 40$  min.<sup>81</sup> Assuming an NO half-life of 1 s, a partition ratio of  $\sim 2400$  would result in equal steady state NO and nitrosothiol concentrations and is within 1 order of magnitude of the determined partition ratio of  $\sim 22000$ . Because iNOS produces low micromolar NO concentrations and current estimates of cellular nitrosothiol concentrations generally fall within the nanomolar range,<sup>20</sup> the determined partition ratio is consistent with iNOS S-nitrosation being responsible, at least in part, for the physiological generation of nitrosothiols. However, future work is needed to determine if the primary function of iNOS S-nitrosation is as a mechanism to control iNOS activity or as an initial source of nitrosothiols. Furthermore, future work is needed to determine what proteins, if any, are direct targets of iNOS transnitrosation.

While the partition ratio between NO release and iNOS S-nitrosation favors NO release for iNOS, eNOS and nNOS might favor S-nitrosation. eNOS and nNOS are more susceptible to inactivation by NO,<sup>31,33,36</sup> suggesting greater S-nitrosation of the constitutive NOS isoforms. In addition, S-nitrosation of eNOS and nNOS might be less coupled to dimer dissociation, allowing transnitrosation reactions to occur without dimer dissociation and inactivation. Consistent with this hypothesis, S-nitrosated eNOS is mostly dimeric, and both eNOS S-nitrosation and inactivation were fully reversible within endothelial cells.<sup>10</sup> In vitro, the eNOS oxidase domain forms the most stable dimer, followed by nNOS and then iNOS.<sup>82</sup> However, further studies are needed to determine the partition ratio between NO release and the S-nitrosation–inactivation process for the constitutive NOS isoforms.

As intracellular GSH concentrations range from 0.5 to 10 mM,<sup>17</sup> GSNO is likely a major product of transnitrosation reactions with S-nitrosated NOS. NOS has been shown to produce nanomolar to low micromolar GSNO concentrations in vitro,<sup>83</sup> in cells,<sup>19</sup> and in plasma.<sup>20,83,84</sup> On the basis of the results in Figure 3, an intracellular GSH concentration of  $\sim 3$  mM approximately doubles  $[\text{NO}]_\infty$  and halves the iNOS autoinactivation rate. This suggests that approximately equal GSNO and S-nitrosated iNOS concentrations are formed at 3 mM GSH. The balance between GSNO formation and iNOS S-nitrosation will favor iNOS S-nitrosation if GSH levels are decreased and favor GSNO if GSH levels are increased. Thus, protein transnitrosation reactions with S-nitrosated iNOS or GSNO might directly respond to GSH levels as well as the cellular redox state (Figure 7B).

In summary, iNOS S-nitrosation plays an important role in the control of NO concentrations and potentially as an initial source of nitrosothiols in vivo. Whether NOS S-nitrosation initiates protein transnitrosation signaling pathways analogous to phosphoryl transfer<sup>16</sup> is an interesting avenue for future work. A complete understanding of the molecular details

involved in the initial formation and transfer of nitrosothiols by NOS might lead to treatments of a broad spectrum of diseases, including cancer, diabetes, and other cardiovascular, pulmonary, and neurological disorders.<sup>4</sup>

## ■ ASSOCIATED CONTENT

### Supporting Information

Further results and discussion of the relevance of alternative proposed mechanisms of NOS autoinactivation besides S-nitrosation, plot of  $[\text{NO}]_\infty$  versus iNOS concentration (Figure S1), chemical structures of a protein nitrosothiol, GSNO,  $N_5$ -nitrosated  $\text{H}_4\text{B}$ , and  $N$ -nitrosomorpholine (Figure S2), and plot of  $[\text{NO}]_\infty$  versus Arg concentration (Figure S3). This material is available free of charge via the Internet at <http://pubs.acs.org>.

## ■ AUTHOR INFORMATION

### Corresponding Author

\*The Scripps Research Institute, 10550 N. Torrey Pines Rd., BCC-529, La Jolla, CA 92037. Telephone: (858) 784-8800. Fax: (858) 784-8801. E-mail: [marletta@scripps.edu](mailto:marletta@scripps.edu).

### Funding

Financial support was provided by GM080272 (M.A.M.) the Aldo DeBenedictis Fund of the University of California, Berkeley, and a National Institute of General Medical Sciences Postdoctoral Fellowship 5F32GM095023 (B.C.S.).

## ■ ACKNOWLEDGMENTS

This project originated from discussion with Dr. Douglas Mitchell and Dr. Joshua Woodward, who made the initial observation of the NOS tunnel. Additionally, we thank members of the Marletta lab for discussions and critical reading of the manuscript.

## ■ ABBREVIATIONS

cGMP, cyclic guanosine monophosphate; GSH, glutathione; GSNO, S-nitrosoglutathione;  $\beta_2$ ,  $\beta_2$  subunit of soluble guanylate cyclase;  $\text{H}_4\text{B}$ , tetrahydrobiopterin; H-NOX, heme nitric oxide and/or oxygen binding domain; HEPES, 4-(2-hydroxyethyl)-1-piperazineethanesulfonic acid;  $\text{HbO}_2$ , oxyhemoglobin; Mb, myoglobin;  $\text{MbO}_2$ , oxymyoglobin; metMb, metmyoglobin; NADPH,  $\beta$ -nicotinamide adenine dinucleotide 2'-phosphate, reduced form; NO, nitric oxide; NOS, nitric oxide synthase; eNOS, endothelial nitric oxide synthase; iNOS, inducible nitric oxide synthase; nNOS, neuronal nitric oxide synthase; sGC, soluble guanylate cyclase; SNAP, S-nitroso-N-acetyl-penicillamine; SNO, S-nitrosothiol; SOD, superoxide dismutase; TCEP, tris(2-carboxyethyl)phosphine.

## ■ ADDITIONAL NOTES

<sup>a</sup>Because  $\text{MbO}_2$  serves as the spectral readout for NO production, it was necessary to maintain a low concentration of  $\text{MbO}_2$  in activity assays.

<sup>b</sup>The interference of GSH was likely due to reduction of the metMb formed upon reaction of NO with  $\text{MbO}_2$ . The reduced Mb can then rebind  $\text{O}_2$  to re-form  $\text{MbO}_2$ , which results in an increase in the apparent inactivation rate.

<sup>c</sup>The magnitude of the inactivation rates titrating  $\beta_2$  H-NOX cannot be directly compared to those with  $\text{MbO}_2$  because of the presence of four cysteines in  $\beta_2$  H-NOX that may alter apparent inactivation rates and the fact that binding of NO to  $\beta_2$  H-NOX is reversible whereas reaction of NO with  $\text{MbO}_2$  is irreversible.



# REFERENCES

- (1) Marletta, M. A., Hurshman, A. R., and Rusche, K. M. (1998) Catalysis by nitric oxide synthase. *Curr. Opin. Chem. Biol.* 2, 656–663.
- (2) Aktan, F. (2004) iNOS-mediated nitric oxide production and its regulation. *Life Sci.* 75, 639–653.
- (3) Derbyshire, E. R., and Marletta, M. A. (2009) Biochemistry of soluble guanylate cyclase. *Handb. Exp. Pharmacol.*, 17–31.
- (4) Foster, M. W., Hess, D. T., and Stamler, J. S. (2009) Protein S-nitrosylation in health and disease: A current perspective. *Trends Mol. Med.* 15, 391–404.
- (5) Basu, S., Kesler, A., Azarova, N. A., Nwanze, N., Perlegas, A., Shiva, S., Broniowska, K. A., Hogg, N., and Kim-Shapiro, D. B. (2010) A novel role for cytochrome c: Efficient catalysis of S-nitrosothiol formation. *Free Radical Biol. Med.* 48, 255–263.
- (6) Broniowska, K. A., Kesler, A., Basu, S., Kim-Shapiro, D. B., and Hogg, N. (2011) Cytochrome c-mediated formation of S-nitrosothiol in cells. *Biochem. J.*, doi: 10.1042/BJ20111294.
- (7) Ravi, K., Brennan, L. A., Levic, S., Ross, P. A., and Black, S. M. (2004) S-nitrosylation of endothelial nitric oxide synthase is associated with monomerization and decreased enzyme activity. *Proc. Natl. Acad. Sci. U.S.A.* 101, 2619–2624.
- (8) Mitchell, D. A., Erwin, P. A., Michel, T., and Marletta, M. A. (2005) S-Nitrosation and regulation of inducible nitric oxide synthase. *Biochemistry* 44, 4636–4647.
- (9) Erwin, P. A., Mitchell, D. A., Sartoretto, J., Marletta, M. A., and Michel, T. (2006) Subcellular targeting and differential S-nitrosylation of endothelial nitric-oxide synthase. *J. Biol. Chem.* 281, 151–157.
- (10) Erwin, P. A., Lin, A. J., Golan, D. E., and Michel, T. (2005) Receptor-regulated dynamic S-nitrosylation of endothelial nitric-oxide synthase in vascular endothelial cells. *J. Biol. Chem.* 280, 19888–19894.
- (11) Jaffrey, S. R., and Snyder, S. H. (2001) The biotin switch method for the detection of S-nitrosylated proteins. *Sci. STKE* 86, p11-9.
- (12) Kim, S. F., Huri, D. A., and Snyder, S. H. (2005) Inducible nitric oxide synthase binds, S-nitrosylates, and activates cyclooxygenase-2. *Science* 310, 1966–1970.
- (13) Matsumoto, A., Comatas, K. E., Liu, L., and Stamler, J. S. (2003) Screening for nitric oxide-dependent protein-protein interactions. *Science* 301, 657–661.
- (14) Mannick, J. B., Hausladen, A., Liu, L., Hess, D. T., Zeng, M., Miao, Q. X., Kane, L. S., Gow, A. J., and Stamler, J. S. (1999) Fas-induced caspase denitrosylation. *Science* 284, 651–654.
- (15) Dunn, J., Gutbrod, S., Webb, A., Pak, A., Jandu, S. K., Bhunia, A., Berkowitz, D. E., and Santhanam, L. (2011) S-nitrosation of arginase 1 requires direct interaction with inducible nitric oxide synthase. *Mol. Cell. Biochem.* 355, 83–89.
- (16) Schaller, G. E., Shiu, S.-H., and Armitage, J. P. (2011) Two-component systems and their co-option for eukaryotic signal transduction. *Curr. Biol.* 21, R320–R330.
- (17) Meister, A., and Anderson, M. E. (1983) Glutathione. *Annu. Rev. Biochem.* 52, 711–760.
- (18) Yap, L.-P., Sancheti, H., Ybanez, M. D., Garcia, J., Cadenas, E., and Han, D. (2010) Determination of GSH, GSSG, and GSNO Using HPLC with Electrochemical Detection. *Methods Enzymol.* 473, 137–147.
- (19) Kluge, I., Gutteck-Amsler, U., Zollinger, M., and Do, K. Q. (1997) S-nitrosoglutathione in rat cerebellum: Identification and quantification by liquid chromatography-mass spectrometry. *J. Neurochem.* 69, 2599–2607.
- (20) Giustarini, D., Milzani, A., Dalle-Donne, I., and Rossi, R. (2007) Detection of S-nitrosothiols in biological fluids: A comparison among the most widely applied methodologies. *J. Chromatogr. B: Anal. Technol. Biomed. Life Sci.* 851, 124–139.
- (21) Mitchell, D. A., and Marletta, M. A. (2005) Thioredoxin catalyzes the S-nitrosation of the caspase-3 active site cysteine. *Nat. Chem. Biol.* 1, 154–158.
- (22) Barglow, K. T., Knutson, C. G., Wishnok, J. S., Tannenbaum, S. R., and Marletta, M. A. (2011) Site-specific and redox-controlled S-nitrosation of thioredoxin. *Proc. Natl. Acad. Sci. U.S.A.* 108, E600–E606.
- (23) Rusche, K. M., Spiering, M. M., and Marletta, M. A. (1998) Reactions catalyzed by tetrahydrobiopterin-free nitric oxide synthase. *Biochemistry* 37, 15503–15512.
- (24) Karow, D. S., Pan, D., Davis, J. H., Behrends, S., Mathies, R. A., and Marletta, M. A. (2005) Characterization of Functional Heme Domains from Soluble Guanylate Cyclase. *Biochemistry* 44, 16266–16274.
- (25) Bradford, M. M. (1976) A rapid and sensitive method for the quantitation of microgram quantities of protein utilizing the principle of protein-dye binding. *Anal. Biochem.* 72, 248–254.
- (26) Hevel, J. M., and Marletta, M. A. (1994) Nitric-oxide synthase assays. *Methods Enzymol.* 233, 250–258.
- (27) Antonini, E., and Brunori, M. (1971) *Hemoglobin and Myoglobin in Their Reactions with Ligands*, North-Holland, Amsterdam.
- (28) Teale, F. (1959) Cleavage of the haem-protein link by acid methylethylketone. *Biochim. Biophys. Acta* 35, 543–543.
- (29) Paulson, D. R., Addison, A. W., Dolphin, D., and James, B. R. (1979) Preparation of ruthenium(II) and ruthenium(III) myoglobin and the reaction of dioxygen, and carbon monoxide, with ruthenium(II) myoglobin. *J. Biol. Chem.* 254, 7002–7006.
- (30) Rosenfeld, R. J., Bonaventura, J., Szymczyna, B. R., Maccoss, M. J., Arvai, A. S., Yates, J. R., Tainer, J. A., and Getzoff, E. D. (2010) Nitric-oxide Synthase Forms N-NO-pterin and S-NO-Cys: Implications for activity, allostery, and regulation. *J. Biol. Chem.* 285, 31581–31589.
- (31) Buga, G. M., Griscavage, J. M., Rogers, N. E., and Ignarro, L. J. (1993) Negative feedback regulation of endothelial cell function by nitric oxide. *Circ. Res.* 73, 808–812.
- (32) Rengasamy, A., and Johns, R. A. (1993) Regulation of nitric oxide synthase by nitric oxide. *Mol. Pharmacol.* 44, 124–128.
- (33) Rogers, N. E., and Ignarro, L. J. (1992) Constitutive nitric oxide synthase from cerebellum is reversibly inhibited by nitric oxide formed from L-arginine. *Biochem. Biophys. Res. Commun.* 189, 242–249.
- (34) Kotsonis, P., Frey, A., Fröhlich, L. G., Hofmann, H., Reif, A., Wink, D. A., Feelisch, M., and Schmidt, H. H. (1999) Autoinhibition of neuronal nitric oxide synthase: Distinct effects of reactive nitrogen and oxygen species on enzyme activity. *Biochem. J.* 340 (Part 3), 745–752.
- (35) Hofmann, H., and Schmidt, H. H. (1995) Thiol dependence of nitric oxide synthase. *Biochemistry* 34, 13443–13452.
- (36) Griscavage, J. M., Rogers, N. E., Sherman, M. P., and Ignarro, L. J. (1993) Inducible nitric oxide synthase from a rat alveolar macrophage cell line is inhibited by nitric oxide. *J. Immunol.* 151, 6329–6337.
- (37) Garrido-del Solo, C., García-Cánovas, F., Havsteen, B. H., and Varón-Castellanos, R. (1993) Kinetic analysis of a Michaelis-Menten mechanism in which the enzyme is unstable. *Biochem. J.* 294 (Part 2), 459–464.
- (38) Varón, R., García-Cánovas, F., García-Moreno, M., Valero, E., Molina-Alarcón, M., García-Meseguer, M. J., Vidal de Labra, J. A., and Garrido-del Sol, C. (2002) Kinetic analysis of the general modifier mechanism of Botts and Morales involving a suicide substrate. *J. Theor. Biol.* 218, 355–374.
- (39) Duggleby, R. G. (1986) Progress curves of reactions catalyzed by unstable enzymes. A theoretical approach. *J. Theor. Biol.* 123, 67–80.
- (40) Burke, M. A., Maini, P. K., and Murray, J. D. (1990) On the kinetics of suicide substrates. *Biophys. Chem.* 37, 81–90.
- (41) Tatsunami, S., Yago, N., and Hosoe, M. (1981) Kinetics of suicide substrates steady-state treatments and computer-aided exact solutions. *Biochim. Biophys. Acta* 662, 226–235.
- (42) Tudela, J., García Cánovas, F., Varón, R., García Carmona, F., Gálvez, J., and Lozano, J. A. (1987) Transient-phase kinetics of enzyme inactivation induced by suicide substrates. *Biochim. Biophys. Acta* 912, 408–416.
- (43) Waley, S. G. (1991) The kinetics of substrate-induced inactivation. *Biochem. J.* 279 (Part 1), 87–94.



- (44) Eich, R. F., Li, T., Lemon, D. D., Doherty, D. H., Curry, S. R., Aitken, J. F., Mathews, A. J., Johnson, K. A., Smith, R. D., Phillips, G. N., and Olson, J. S. (1996) Mechanism of NO-induced oxidation of myoglobin and hemoglobin. *Biochemistry* 35, 6976–6983.
- (45) Stuehr, D. J., Kwon, N. S., and Nathan, C. F. (1990) FAD and GSH participate in macrophage synthesis of nitric oxide. *Biochem. Biophys. Res. Commun.* 168, 558–565.
- (46) Harbrecht, B. G., Di Silvio, M., Chough, V., Kim, Y. M., Simmons, R. L., and Billiar, T. R. (1997) Glutathione regulates nitric oxide synthase in cultured hepatocytes. *Ann. Surg.* 225, 76–87.
- (47) Komori, Y., Hyun, J., Chiang, K., and Fukuto, J. M. (1995) The role of thiols in the apparent activation of rat brain nitric oxide synthase (NOS). *J. Biochem.* 117, 923–927.
- (48) Martin, N. I., Woodward, J. J., Winter, M. B., and Marletta, M. A. (2009) 4,4-Difluorinated analogues of L-arginine and N(G)-hydroxy-L-arginine as mechanistic probes for nitric oxide synthase. *Bioorg. Med. Chem. Lett.* 19, 1758–1762.
- (49) Ravichandran, L. V., Johns, R. A., and Rengasamy, A. (1995) Direct and reversible inhibition of endothelial nitric oxide synthase by nitric oxide. *Am. J. Physiol.* 268, H2216–H2223.
- (50) Roman, L. J., Miller, R. T., de la Garza, M. A., Kim, J. J., and Siler Masters, B. S. (2000) The C terminus of mouse macrophage inducible nitric-oxide synthase attenuates electron flow through the flavin domain. *J. Biol. Chem.* 275, 21914–21919.
- (51) Wei, C. C., Wang, Z. Q., Wang, Q., Meade, A. L., Hille, R., and Stuehr, D. J. (2001) Rapid kinetic studies link tetrahydrobiopterin radical formation to heme-dioxy reduction and arginine hydroxylation in inducible nitric-oxide synthase. *J. Biol. Chem.* 276, 315–319.
- (52) Wang, Z.-Q., Wei, C.-C., and Stuehr, D. J. (2002) A conserved tryptophan 457 modulates the kinetics and extent of N-hydroxy-L-arginine oxidation by inducible nitric-oxide synthase. *J. Biol. Chem.* 277, 12830–12837.
- (53) Wang, Z. Q., Wei, C. C., Ghosh, S., Meade, A. L., Hille, R., and Stuehr, D. J. (2001) A conserved tryptophan in nitric oxide synthase regulates heme-dioxy reduction by tetrahydrobiopterin. *Biochemistry* 40, 12819–12825.
- (54) Lefèvre-Groboillot, D., Boucher, J.-L., Mansuy, D., and Stuehr, D. J. (2006) Reactivity of the heme-dioxygen complex of the inducible nitric oxide synthase in the presence of alternative substrates. *FEBS J.* 273, 180–191.
- (55) Zhao, Y., Brandish, P. E., Ballou, D. P., and Marletta, M. A. (1999) A molecular basis for nitric oxide sensing by soluble guanylate cyclase. *Proc. Natl. Acad. Sci. U.S.A.* 96, 14753–14758.
- (56) Assreuy, J., Cunha, F. Q., Liew, F. Y., and Moncada, S. (1993) Feedback inhibition of nitric oxide synthase activity by nitric oxide. *Br. J. Pharmacol.* 108, 833–837.
- (57) Sheehy, A. M., Burson, M. A., and Black, S. M. (1998) Nitric oxide exposure inhibits endothelial NOS activity but not gene expression: A role for superoxide. *Am. J. Physiol.* 274, L833–L841.
- (58) Ma, X. L., Lopez, B. L., Christopher, T. A., Birenbaum, D. S., and Vinten-Johansen, J. (1996) Exogenous NO inhibits basal NO release from vascular endothelium in vitro and in vivo. *Am. J. Physiol.* 271, H2045–H2051.
- (59) Taldone, F. S., Tummala, M., Goldstein, E. J., Ryzhov, V., Ravi, K., and Black, S. M. (2005) Studying the S-nitrosylation of model peptides and eNOS protein by mass spectrometry. *Nitric Oxide* 13, 176–187.
- (60) Keszler, A., Zhang, Y., and Hogg, N. (2010) Reaction between nitric oxide, glutathione, and oxygen in the presence and absence of protein: How are S-nitrosothiols formed? *Free Radical Biol. Med.* 48, 55–64.
- (61) Keshive, M., Singh, S., Wishnok, J. S., Tannenbaum, S. R., and Deen, W. M. (1996) Kinetics of S-nitrosation of thiols in nitric oxide solutions. *Chem. Res. Toxicol.* 9, 988–993.
- (62) Madej, E., Folkes, L. K., Wardman, P., Czapski, G., and Goldstein, S. (2008) Thiyl radicals react with nitric oxide to form S-nitrosothiols with rate constants near the diffusion-controlled limit. *Free Radical Biol. Med.* 44, 2013–2018.
- (63) Lim, C. H., Dedon, P. C., and Deen, W. M. (2008) Kinetic analysis of intracellular concentrations of reactive nitrogen species. *Chem. Res. Toxicol.* 21, 2134–2147.
- (64) Slama-Schwok, A., Nègrerie, M., Berka, V., Lambry, J.-C., Tsai, A.-L., Vos, M. H., and Martin, J.-L. (2002) Nitric oxide (NO) traffic in endothelial NO synthase. Evidence for a new NO binding site dependent on tetrahydrobiopterin? *J. Biol. Chem.* 277, 7581–7586.
- (65) Lakowicz, J. R., and Weber, G. (1973) Quenching of protein fluorescence by oxygen. Detection of structural fluctuations in proteins on the nanosecond time scale. *Biochemistry* 12, 4171–4179.
- (66) Pant, K., and Crane, B. R. (2006) Nitrosyl–Heme Structures of *Bacillus subtilis* Nitric Oxide Synthase Have Implications for Understanding Substrate Oxidation. *Biochemistry* 45, 2537–2544.
- (67) Möller, M. N., Li, Q., Lancaster, J. R., and Denicola, A. (2007) Acceleration of nitric oxide autooxidation and nitrosation by membranes. *IUBMB Life* 59, 243–248.
- (68) Keller, G. A., Barke, R., Harty, J. T., Humphrey, E., and Simmons, R. L. (1985) Decreased hepatic glutathione levels in septic shock. Predisposition of hepatocytes to oxidative stress: An experimental approach. *Arch. Surg.* 120, 941–945.
- (69) Okabe, H., Irita, K., Taniguchi, S., Kurosawa, K., Tagawa, K., Yoshitake, J., and Takahashi, S. (1994) Endotoxin causes early changes in glutathione concentrations in rabbit plasma and liver. *J. Surg. Res.* 57, 416–419.
- (70) McKelvey, T. G., Höllwarth, M. E., Granger, D. N., Engerson, T. D., Landler, U., and Jones, H. P. (1988) Mechanisms of conversion of xanthine dehydrogenase to xanthine oxidase in ischemic rat liver and kidney. *Am. J. Physiol.* 254, G753–G760.
- (71) Hotherhall, J. S., Cunha, F. Q., Neild, G. H., and Norohna-Dutra, A. A. (1997) Induction of nitric oxide synthesis in J774 cells lowers intracellular glutathione: Effect of modulated glutathione redox status on nitric oxide synthase induction. *Biochem. J.* 322 (Part 2), 477–481.
- (72) Buchmuller-Rouiller, Y., Corradin, S. B., Smith, J., Schneider, P., Ransijn, A., Jongeneel, C. V., and Mauël, J. (1995) Role of Glutathione in Macrophage Activation: Effect of Cellular Glutathione Depletion on Nitrite Production and Leishmanicidal Activity. *Cell. Immunol.* 164, 73–80.
- (73) Tirmenstein, M. A., Nicholls-Grzemeski, F. A., Schmittgen, T. D., Zakrajsek, B. A., and Fariss, M. W. (2000) Glutathione-dependent regulation of nitric oxide production in isolated rat hepatocyte suspensions. *Antioxid. Redox Signaling* 2, 767–777.
- (74) Ghigo, D., Alessio, P., Foco, A., Bussolino, F., Costamagna, C., Heller, R., Garbarino, G., Pescarmona, G. P., and Bosia, A. (1993) Nitric oxide synthesis is impaired in glutathione-depleted human umbilical vein endothelial cells. *Am. J. Physiol.* 265, C728–C732.
- (75) Murphy, M. E., Piper, H. M., Watanabe, H., and Sies, H. (1991) Nitric oxide production by cultured aortic endothelial cells in response to thiol depletion and replenishment. *J. Biol. Chem.* 266, 19378–19383.
- (76) Laursen, J. B., Boesgaard, S., Trautner, S., Rubin, L., Poulsen, H. E., and Aldershvile, J. (2001) Endothelium-dependent vasorelaxation is inhibited by in vivo depletion of vascular thiol levels: Role of endothelial nitric oxide synthase. *Free Radical Res.* 35, 387–394.
- (77) Sugiyama, T., and Michel, T. (2010) Thiol-metabolizing proteins and endothelial redox state: Differential modulation of eNOS and biopterin pathways. *Am. J. Physiol.* 298, H194–H201.
- (78) Song, M., Kellum, J. A., Kaldas, H., and Fink, M. P. (2004) Evidence that glutathione depletion is a mechanism responsible for the anti-inflammatory effects of ethyl pyruvate in cultured lipopolysaccharide-stimulated RAW 264.7 cells. *J. Pharmacol. Exp. Ther.* 308, 307–316.
- (79) Liu, X., Miller, M. J., Joshi, M. S., Sadowska-Krowicka, H., Clark, D. A., and Lancaster, J. R. (1998) Diffusion-limited reaction of free nitric oxide with erythrocytes. *J. Biol. Chem.* 273, 18709–18713.
- (80) Thomas, D. D., Liu, X., Kantrow, S. P., and Lancaster, J. R. (2001) The biological lifetime of nitric oxide: Implications for the perivascular dynamics of NO and O<sub>2</sub>. *Proc. Natl. Acad. Sci. U.S.A.* 98, 355–360.

- (81) Stamler, J. S., Simon, D. I., Osborne, J. A., Mullins, M. E., Jaraki, O., Michel, T., Singel, D. J., and Loscalzo, J. (1992) S-nitrosylation of proteins with nitric oxide: Synthesis and characterization of biologically active compounds. *Proc. Natl. Acad. Sci. U.S.A.* 89, 444–448.
- (82) Panda, K., Rosenfeld, R. J., Ghosh, S., Getzoff, E. D., and Stuehr, D. J. (2002) Distinct dimer interaction and regulation in nitric-oxide synthase types I, II, and III. *J. Biol. Chem.* 277, 31020–31030.
- (83) Mayer, B., Pfeiffer, S., Schrammel, A., Koesling, D., Schmidt, K., and Brunner, F. (1998) A new pathway of nitric oxide/cyclic GMP signaling involving S-nitrosoglutathione. *J. Biol. Chem.* 273, 3264–3270.
- (84) Tsikas, D. (2000) Is S-nitrosoglutathione formed in nitric oxide synthase incubates? *FEBS Lett.* 483, 83–84.
- (85) Crane, B. R., Arvai, A. S., Ghosh, S., Getzoff, E. D., Stuehr, D. J., and Tainer, J. A. (2000) Structures of the N<sup>ω</sup>-hydroxy-L-arginine complex of inducible nitric oxide synthase oxygenase dimer with active and inactive pterins. *Biochemistry* 39, 4608–4621.
- (86) Beneš, P., Chovancová, E., Kozlíková, B., Pavelka, A., Strnad, O., Brezovský, J., Sustr, V., Klvaňa, M., Szabó, T., Gora, A., Zamborský, M., Biedermannová, L., Medek, P., Damborský, J., and Sochor, J. (2010) CAVER, version 2.1.